Electrochemical behaviour of *N*-acetyl-L-cysteine on gold electrode—A tentative reaction mechanism

C. Barus [a,*], P. Gros [a], M. Comtat [a], S. Daunes-Marion [b], R. Tarroux [b]

[a] *Laboratoire de Génie Chimique, UMR 5503, Université Paul Sabatier, Département Procédés Electrochimiques, 31062 Toulouse Cedex 9, France*

[b] *Société Pierre Fabre Dermo-Cosmétique, Service Pharmocochimie, Allée Camille Soula, Vigoulet Auzil, BP 74, 31322 Castanet Tolosan, France*

Abstract

The electrochemical behaviour of *N*-acetyl-L-cysteine (NAC) has been investigated by linear and cyclic voltammetry on gold electrode at room temperature. The results showed two oxidation peaks under acid and neutral conditions and only one in basic medium. For each oxidation, as many electron was exchanged as proton. The influence of both the concentration and the potential scan rate on the peak currents highlighted a diffusion-controlled phenomenon for the first peak and an adsorption-limited reaction rate for the second one. The diffusion coefficient of NAC in solution and the surface concentration of the adsorbed species at pH 3 and 7 were close to 2×10^{-4} to 2×10^{-5} cm^2 s^{-1} and 6×10^{-9} to 6×10^{-10} mol cm^{-2}, respectively. Film transfer experiments resulted in an irreversible adsorption of NAC on gold electrode, and the formation of a self-assembled monolayer (SAM).

Keywords: *N*-Acetyl-L-cysteine; Cyclic voltammetry; Adsorption; Thiols; Oxidation mechanism

1. Introduction

N-Acetyl-L-cysteine (NAC) is an acetylated derivative of the amino acid L-cysteine. NAC is commonly used as pharmaceutics. It has first been managed as a mucolytic agent reducing the viscosity of pulmonary secretions in chronic respiratory illness as well as an antidote for hepatotoxicity due to acetaminophen overdose. It has also been efficient in the treatment of Sjogren's syndrome, smoking cessation, influenza, hepatitis C, and myoclonus epilepsy [1]. Another less expanded chemical property of NAC concerns its antioxidant activity. As a matter of fact, NAC constitutes an excellent source of sulphydryl groups (SH) converted in organism into metabolites able to stimulate the synthesis of reduced glutathione (GSH). It also acts as a scavenger of free radicals and reactive oxygen species (ROS), consuming directly superoxide anion [2] or hypochlorous acid [3]. This reactivity makes NAC a powerful antioxidant and a potentially therapeutic agent in the treatment of cancer [4], cardiovascular and respiratory diseases [5], human immunodeficiency virus (HIV) infection [6,7], acetaminophen toxicity [8], neurodegenerative disorder [9] and other diseases characterized by free radicals production and oxidative damage.

Its antioxidant properties give to NAC a significant role against oxidative stress, particularly in conditions characterized by the decrease of GSH concentration [10]. Oxidative stress is often associated to the massive generation of ROS [11,12]. Consequences on organism are multiple (cancers, psoriasis, ageing, etc.) [13,14]. NAC antioxidant activity and its aptitude to reduce oxidative stress open new applications. Like other reducing molecules (Vitamins A, C, E, etc.), NAC could, for instance, show antioxidant efficiency in dermocosmetic creams used to avoid cutaneous ageing. Electrochemistry represents a well-defined methodology to study redox properties of antioxidant species, in model solution as well as in complex media. Previous works performed in the laboratory have shown possibilities to evaluate the antioxidant capacity of various media such as wine [15], skin [16], or dermocosmetic creams [17], by simple electrochemical measurements. Furthermore it has also been

possible to determine and sometimes quantify the major redox markers involved without any pre-treatment of the sample. In this context the determination of the electrochemical properties of NAC in solution is essential to project its future integration in complex media like galenics.

Electrochemical study of thiols gave rise to several publications on the mechanism of cysteine oxidation on platinum and gold electrodes. However most of works induced disparate and even contradictory experimental data, resulting in divergent interpretations [18–20]. Few works dealt with the electrochemistry of NAC itself. The oxidation of NAC at glassy carbon electrode gives a very poor electrochemical response [21], while thiols oxidation is very complex at mercury, gold and platinum electrodes [22]. In order to propose a specific electrochemical detection, different chemically modified carbon electrodes were developed [21,23], as well as the use of a mediator [24]. In this paper we preferred to use bare gold electrode because of the strong adsorption of sulphur atom on such material.

2. Material and methods

2.1. Chemicals

Sulphuric acid (H_2SO_4) 95% (w/v), potassium dihydrogenophosphate (KH_2PO_4), di-potassium hydrogenophosphate (K_2HPO_4) and NAC were purchased from Acros Organics. Otherwise indicated, the electrolytic solutions were prepared in phosphate solution 0.1 mol L^{-1} just before the experiments. pH was adjusted by addition of sulphuric acid or sodium hydroxide.

2.2. Electrochemistry

Electrochemical manipulations were performed at constant room temperature (298 K) with an Autolab Metrohm potentiostat interfaced to an HP omni-book XE 4500 microcomputer and using the GPES 4.9 software. A three-electrode system was used for all the experiments. Two gold disk were used as working electrodes. The surface area of the first electrode, used for cyclic voltammetry measurements, was 0.071 cm^2. The second electrode was a rotating disk electrode (surface area: 0.0314 cm^2) and was used for experiments in steady state conditions. The later was connected to a Speed Control Unit CTV 101 from Radiometer. Platinum grid acted as counter electrode and the reference electrode was a saturated calomel electrode (SCE) (Hg/Hg_2Cl_2, KCl_{sat}), connected to the cell by a Luggin capillary. All potentials were expressed versus this electrode.

Before the electrochemical measurements, all solutions were deaerated by bubbling nitrogen for 10 min. The potential range was chosen in order to avoid oxidation and reduction of water.

The background current was systematically recorded by plotting the current–potential curve with the supporting electrolyte only. To optimize the exploitation of the numerical data, the background was subtracted from the overall experimental curves by using GPES software. When two close anodic signals were present, peaks were deconvoluted using the Microcal Origin 7.0 software including the peak fitting module. It consists in a mathematical treatment of the overall signal which is decomposed in a sum of Gaussian peaks associated to each electrochemical reaction [25].

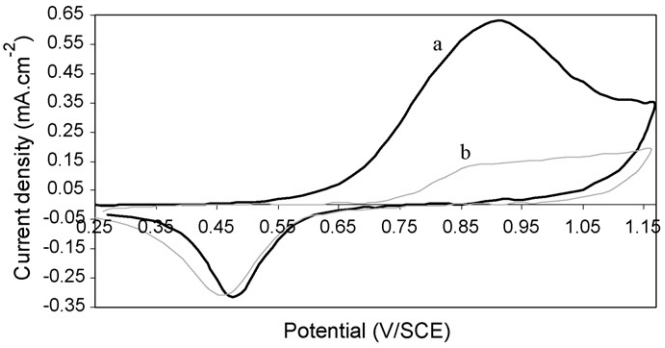

Fig. 1. Cyclic voltammograms on gold electrode of (a) NAC 10^{-3} M in 0.1 M deaerated phosphate buffer pH 7; (b) background current.Potential scan rate: 200 mV s^{-1}.

2.3. Electrode pre-treatment

The gold electrode surface was polished with abrasive paper (262× imperial lapping film sheets) and rinsed with distilled water. Cathodic and anodic polarizations were then performed at −2 and +2 V successively during 30 s in H_2SO_4 0.5 mol L^{-1}. Finally, cyclic voltammograms were carried out in H_2SO_4 0.5 mol L^{-1} at 200 mV s^{-1} between −0.1 and 1.4 V, until obtaining reproducible current–potential curves.

3. Results

Fig. 1 shows the cyclic voltammogram of NAC in phosphate buffer pH 7 (curve a). An anodic peak corresponding to NAC oxidation appeared at about 0.9 V. No cathodic peak was obtained in the reverse scan excepted that observed at 0.47 V corresponding to reduction of gold oxides (curve b). This clearly suggests the strong irreversibility of the reaction. To confirm this result, successive cyclic voltammograms were recorded in the same experimental conditions by increasing gradually the upper potential limit. For values less than 0.9 V, no cathodic peak was detected, although NAC oxidation signal started from 0.65 V. A cathodic peak clearly appeared only for upper potential values higher than 0.9 V (results not shown). Similar results were obtained without NAC dissolved in phosphate buffer, thus proving the electroinactivity of the NAC oxidation product formed during the anodic scan.

Cyclic voltammograms of NAC recorded in various pH phosphate solutions are presented in Fig. 2. In all cases, the background current was subtracted as indicated in Section 2.2. The voltammograms revealed two oxidation peaks (named peak 1 for the lowest potential and peak 2 for the highest) under acid (pH 1.6) and neutral conditions (pH 7) and only one (peak 2) under basic conditions (pH 9 and 12). The influence of pH on the peaks potential has been studied by recording current–potential curves in phosphate solutions with pH ranging from 1.6 to 12. A linear correlation was obtained for both peaks with a slope of 60 mV/pH unit (Fig. 2 inset). This result implies that the num-

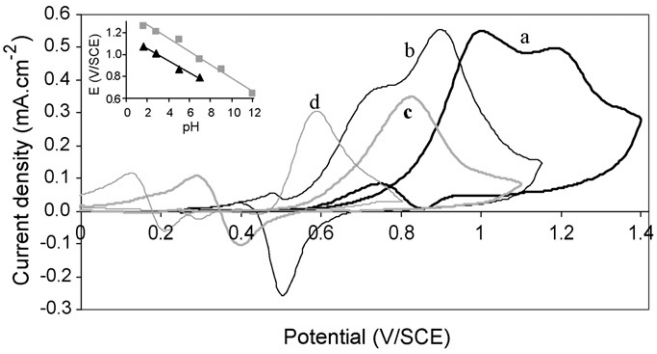

Fig. 2. Cyclic voltammograms on gold electrode of NAC 10^{-3} M in 0.1 M deaerated phosphate solutions at (a) pH 1.6; (b) pH 7; (c) pH 9 and (d) pH 12—potential scan rate: 50 mV s^{-1} (background current subtracted). Inset: variation of peak potential with pH, (▲) peak 1; (■) peak 2.

ber of electron and proton exchanged in each step of the reaction mechanism are the same.

The influence of NAC concentration was studied in phosphate buffer pH 7 in the range 10^{-5} to 10^{-3} mol L^{-1} (Fig. 3). Two evolutions were observed (Fig. 3 inset): for peak 1 (near 0.75 V), the current density increased proportionally to NAC concentration. On the other hand the current recorded for peak 2 (near 0.9 V) was roughly independent of NAC concentration.

The influence of the potential scan rate on the electrochemical response was studied at pH 3 (Fig. 4). The peak current density (i_p) was proportional to the square root of the scan rate for peak 1 (Fig. 5A) whereas it increased linearly with the scan rate for peak 2 (Fig. 5B). These results suggest a diffusion-controlled reaction rate for the first oxidation while the second oxidation is limited by adsorption phenomena. The same results were obtained at pH 7 (results not shown). The diffusion coefficient (D) and the surface concentration (Γ) of the adsorbed species on gold were calculated for both pH. They were deduced from the slope of the previous curves (Fig. 5), according to Eqs. (1) and (2), respectively [26]:

$$i_p = (2.99 \times 10^5) n\alpha^{1/2} D^{1/2} r^{1/2} C \quad (1)$$

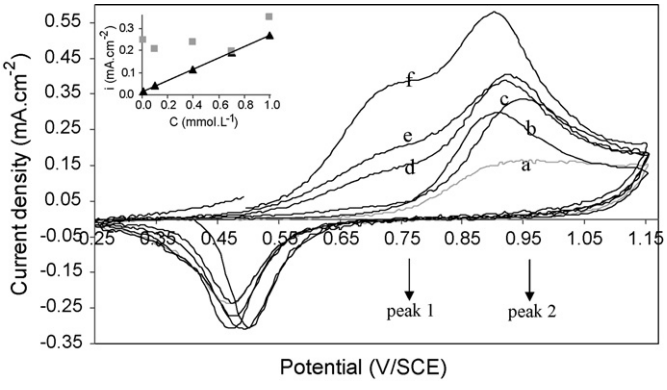

Fig. 3. Cyclic voltammograms of NAC in 0.1 M deaerated phosphate buffer pH 7: (a) background current; (b) 10^{-5} M; (c) 10^{-4} M; (d) 4.10^{-4} M; (e) 7.10^{-4} M and (f) 10^{-3} M—potential scan rate: 50 mV s^{-1}. Inset: variation of current density with NAC concentration, (▲) peak 1; (■) peak 2.

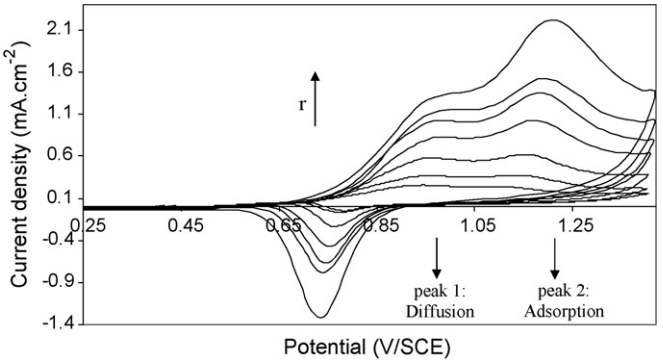

Fig. 4. Cyclic voltammograms of NAC 10^{-3} M in 0.1 M deaerated phosphate solution pH 3—potential scan rate: 10; 25; 50; 100; 150; 200 and 250 mV s^{-1}.

$$i_p = \frac{n\alpha F^2 r\Gamma}{2.718RT} \quad (2)$$

where n is the total number of electrons transferred in the electrochemical reaction (in this case $n = 1$), α the anodic transfer coefficient, C the NAC bulk concentration, r the potential scan rate, F the Faraday constant, R the gas constant and T is the absolute temperature.

α was previously calculated from the difference between the peak potential (E_p) and the half wave potential ($E_{p/2}$) according to Eqs. (3) and (4) related to a diffusion-controlled and an adsorption-limited reaction rate, respectively [26]:

$$\Delta E_{p1} = E_p - E_{p/2} = \frac{47.7}{\alpha}\text{mV} \quad (\text{at } 298\text{ K}) \quad (3)$$

$$\Delta E_{p2} = E_p - E_{p/2} = \frac{62.5}{\alpha}\text{mV} \quad (\text{at } 298\text{ K}) \quad (4)$$

All data are collected in Table 1.

Anodic peak potentials were dependent on the scan rate. Fig. 6 shows that plots of E_p versus $\ln(r)$ are linear at pH 3 (A) and at pH 7 (B), for both peaks. This is in agreement with Nicholson–Shain's equations (5) and (6) for an irreversible electrochemical system in the case of a diffusion-controlled and an adsorption-limited anodic reaction rate, respectively [26]:

$$E_p = E^{\circ\prime} + \frac{RT}{\alpha F}\left[0.780 + \ln\left(\frac{D^{1/2}}{k^\circ}\right) + \ln\left(\frac{\alpha F r}{RT}\right)^{1/2}\right] \quad (5)$$

$$E_p = E^{\circ\prime} - \frac{RT}{\alpha F}\ln\left(\frac{RT}{\alpha F}\frac{k^\circ}{r}\right) \quad (6)$$

Table 1
Values of NAC anodic transfer coefficient (α), diffusion coefficients (D) and surface concentrations (Γ) at pH 3 and 7

	Peak 1 (diffusion-controlled reaction)	Peak 2 (adsorption-limited reaction)
pH 3	$\alpha = 0.34 \pm 0.04$ $D = 2 \times 10^{-4}$ cm^2 s^{-1}	$\alpha = 0.72 \pm 0.14$ $\Gamma = 6 \times 10^{-9}$ mol cm^{-2} 4×10^{15} NAC molecule cm^{-2}
pH 7	$\alpha = 0.32 \pm 0.07$ $D = 2 \times 10^{-5}$ cm^2 s^{-1}	$\alpha = 0.84 \pm 0.07$ $\Gamma = 6 \times 10^{-10}$ mol cm^{-2} 4×10^{14} NAC molecule cm^{-2}

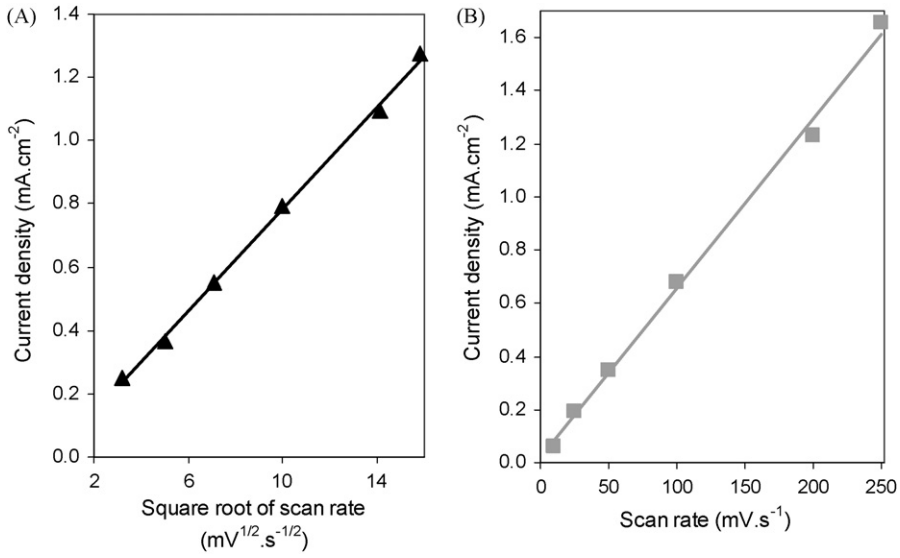

Fig. 5. Evolution of current density with: (A) the square root of the scan rate and (B) the scan rate, (▲) peak 1; (■) peak 2. Same experimental conditions as Fig. 4.

where $E^{\circ\prime}$ is the formal potential and k° is the standard heterogeneous rate constant.

Current–potential curves were plotted in steady state conditions using different electrode rotation rates. Experiments were performed at pH 3 (results no shown) and pH 7 (Fig. 7). Although the solution was stirred, current peaks were observed instead of limit currents, highlighting the complexity of this oxidation. Similar results were obtained for both pH. The electrode reaction rate for the peak 1 was limited by diffusion as previously shown (Fig. 5A). However, Levich's equation, governing convective diffusion phenomenon, did not present a linear relationship (results not shown). On the other hand, reverse of the current density is proportional to the reverse of the square root of the electrode rotation rate (Fig. 7 inset). This evolution is similar to that of the Koutecky–Levich equation (7) and would predict a coupled chemical reaction or a presence of a reaction intermediate in the oxidation mechanism [26]:

$$\frac{1}{i}=\frac{1}{i_K}+\frac{1}{i_l},\quad \text{where } i_K=FCk^{\circ}\exp\left(-\frac{\alpha F}{RT}(E-E^{\circ\prime})\right), \text{ and}$$

$$i_l=0.620nFD^{2/3}\omega^{1/2}\nu^{-1/6}C \tag{7}$$

i_K represents the current density in the absence of any mass-transfer effects. This suggests the existence of a slow step in the electronic transfer reaction. i_l is the limiting current density, ω the angular frequency of electrode rotation and ν is the kinematic viscosity of the solution.

One can note on the current–potential curves of Fig. 7 an anodic peak for the reverse scan. This peak was noticeable only when residual current was subtracted (Fig. 2 for example). It could be explained by the oxidation of NAC on a bare gold surface electrode after the gold oxides reduction, similarly to

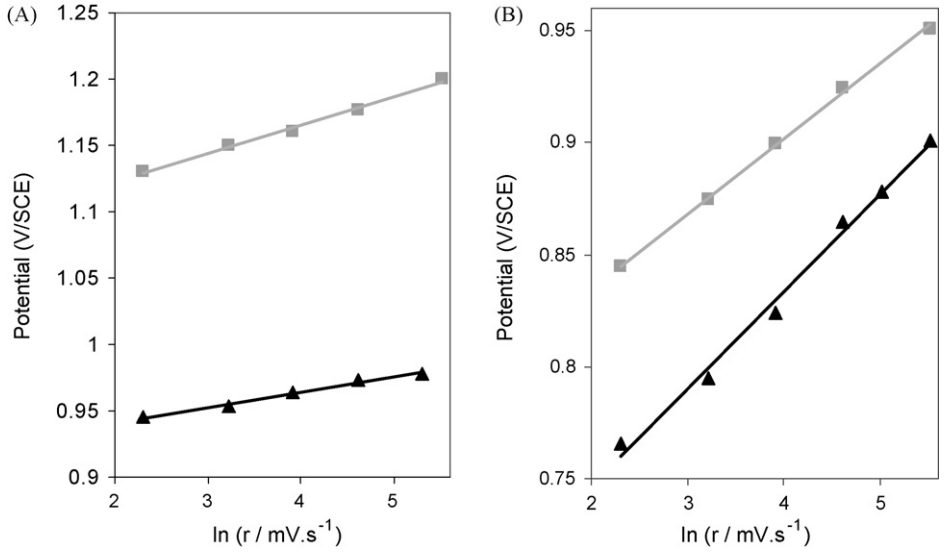

Fig. 6. Evolution of peak potential with the logarithm of potential scan rate: (A) pH 3 and (B) pH 7, (▲) peak 1; (■) peak 2. Other experimental conditions are indicated in Fig. 4.

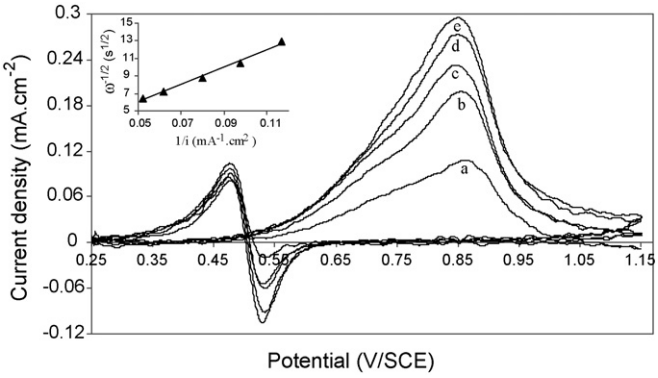

Fig. 7. Current–potential curve of NAC 10^{-4} M in stirred 0.1 M deaerated phosphate buffer pH 7, influence of the gold electrode rotation rate: (a) 700 rpm, (b) 1000 rpm, (c) 1500 rpm, (d) 2500 rpm and (e) 3500 rpm—potential scan rate: 10 mV s^{-1} (background current subtracted). Inset: variation of reverse of current density with reverse of square root of the electrode rotation rate, (▲) peak 1.

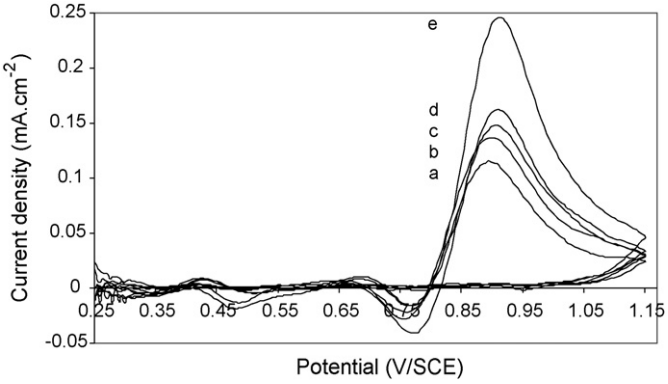

Fig. 9. Cyclic voltammograms of 0.1 M deaerated phosphate buffer pH 7, in function of immersion time of gold electrode in NAC 10^{-3} M solution: (a) 30 s; (b) 1 min; (c) 5 min; (d) 10 min and (e) 16 h—potential scan rate: 50 mV s^{-1} (background current subtracted).

that previously mentioned for the oxidation of cysteine [19]. This anodic peak was more visible in steady state conditions due to the stirring of the solution which allowed a continuous brought of the electroactive species near the electrode surface.

Fig. 8 compares voltammograms obtained at pH 3 with and without stirring the NAC solution. The electrode reaction rate for the first peak being controlled by diffusion, the increase of current density when NAC solution is stirred, was expected. No difference was noted on the peak potential. For the second peak, because of adsorption limitations, stirring the solution did not influence the current density. On the other hand, agitation involved a potential shift of about 100 mV to lower value. The results at pH 7 led to the same observations. So, oxidation of the adsorbed molecule is easier when solution is stirred.

Thiols are molecules known to adsorb on gold surface and several publications indicate adsorption and self-assembled monolayer's (SAM) formation [27–31]. In order to confirm this fact, film transfer experiments were carried out for NAC solutions 10^{-4} and 10^{-3} mol L^{-1} at pH 3 and pH 7 by immersing gold electrode in NAC solution during various times between 30 s and 16 h (no potential was applied). The electrode was then washed with distilled water. Finally, the electrode was transferred to a phosphate solution and cyclic voltammograms were recorded. An electrochemical signal due to NAC oxidation was observed for both pH, even for relatively low immersion times. It should be noted that no peak 1 (diffusion controlled) was observed in the absence of NAC in the bulk solution but only peak 2 (adsorption controlled). Results obtained at pH 7 are given in Fig. 9 showing that NAC is spontaneously adsorbed on gold electrode surface. Even an extensive washing was not sufficient to desorb NAC. This remark confirm that NAC is chemisorbed on gold, by means of irreversible strong interactions, as it was previously mentioned in bibliography [22,32,33].

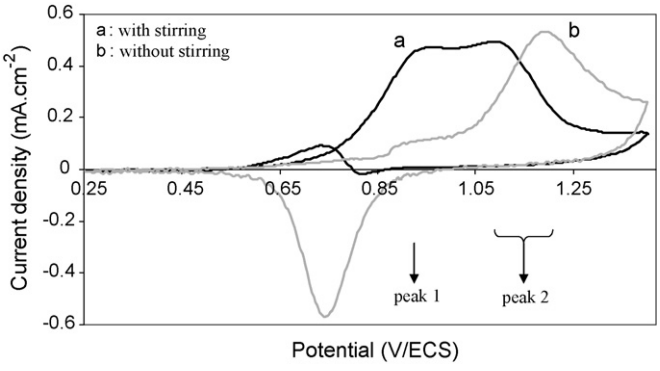

Fig. 8. Cyclic voltammograms of NAC 10^{-4} M in 0.1 M deaerated phosphate solutions pH 3: (a) stirred solution (3500 rpm)—potential scan rate: 10 mV s^{-1} and (b) unstirred solution—potential scan rate: 50 mV s^{-1}.

4. Discussion

NAC oxidation occurred at high potentials and under the experimental conditions used, it was impossible to reduce the resulting compound. The oxidation product is then electroinactive, and no cathodic peak was observed.

Film transfer experiments highlighted spontaneous chemisorption, which results from a strong interaction between the NAC sulphur atoms and gold atoms of the electrode surface. The amount of charge under the current–potential curve (Fig. 9) was correlated to the number of NAC molecules adsorbed. Considering a Au(1 0 0) single-crystal electrode and a monoelectronic transfer, results obtained, for both pH, indicate that the number of adsorbed NAC molecules, between 10^{15} and 6×10^{15} molecules cm^{-2}, was the same order of magnitude than gold atoms number (10^{15} atoms cm^{-2}). These results are in agreement with those obtained above and reported in Table 1. Moreover, no notorious difference appeared whatever the NAC concentration used, e.g. 10^{-4} and 10^{-3} mol L^{-1}. In the experimental conditions adopted, this adsorption phenomenon was not influenced by NAC concentration. All these results consequently suggest a monolayer of NAC adsorbed. However, the size of the NAC molecule is higher than the gold atom one. Moreover, considering the steric hindrance of NAC, it appears impossible to adsorb as many NAC molecules as gold atoms present on the electrode surface. This implies a self-organization in multilayers.

This model has already been proposed by Uvdal et al. in the case of L-cysteine [34]. They suggested a double layer organization, where the second layer partly overlaps the first one, which binds to the surface through the sulphur. The next layer interacts with the chemisorbed layer through the amino and the carboxylate groups by electrostatic interactions. By X-ray photoelectron spectroscopy, it was found that about 50% of the thiol groups were in contact with the metal. Considering the present results, a similar process could be also expected for NAC.

Furthermore, in bibliography, Quartz Crystal Microbalance (QCM) measurements and in situ Infra-Red spectroscopy reveal very fast initial adsorption, followed, after approximately 1 min, by a considerably slower mass uptake [30]. After the initial adsorption step, which should correspond to the chemisorption of the first layer, two processes are observed simultaneously. On one hand, a fraction of the molecules undergoes deprotonation of the carboxylic acid group (COOH), the gold surface playing the role of proton acceptor. On an other hand, results indicate hydrogen-bonding interactions within the SAM, possibly between the acid and the amide groups of adjacent molecules. The orientation of NAC following initial adsorption, favors both the deprotonation of COOH and the intermolecular interactions [30]. This second process agrees completely with the description of the second layer proposed by Uvdal et al. [34]. This model could explain the results obtained in Fig. 9, where the curve (a) corresponded to the fast initial adsorption, and then curves (b) to (e), where the signal increased progressively, illustrated the second step of adsorption.

Such an irreversible NAC adsorption and the electrode surface modifications by SAM may be exploited for analytical applications, for instance dopamine electroanalysis [35]. Cysteine has been also used in this kind of applications [29,36,37].

Passivation phenomenon of electrode surface was also highlighted, depending on adsorption. Experiments carried out under steady state conditions led to current peaks instead of diffusion waves. Also, current density decreased when the number of cycles increased (results not shown), considerably for the second cycle, more slowly for the following cycles.

The anodic peak present on reverse scan (Fig. 7), corresponding to NAC reoxidation, is observed only after reduction of gold oxides formed during the anodic scan, and thus, bare gold surface re-establishment.

The equation for NAC (noted RSH) oxidation may be

$$2\mathrm{RSH} \rightarrow \mathrm{RSSR} + 2\mathrm{H}^+ + 2\mathrm{e}^- \quad (8)$$

corresponding to one electron exchanged for one proton.

The presented results illustrate that the first oxidation peak, at lower potential, is limited by NAC diffusion to the electrode surface. NAC oxidation occurs either, through NAC film adsorbed, or on free surface, according to the reaction:

$$\mathrm{RSH_{sol}} \rightarrow \mathrm{RS^{\bullet}} + \mathrm{H}^+ + \mathrm{e}^- \quad (9)$$

Nevertheless, it can be considered the chemisorption of the radical $\mathrm{RS^{\bullet}}$ on the gold surface:

$$\overset{(-\mathrm{II})}{\mathrm{RSH_{sol}}} + \mathrm{Au} \rightarrow \overset{(-\mathrm{I})}{\mathrm{RS}} - \mathrm{Au} + \mathrm{H}^+ + \mathrm{e}^- \quad (10)$$

On the contrary, the second peak, at higher potential, is controlled by adsorption phenomena. Two adsorption forms exist: NAC chemisorbed in the first layer closed to gold surface and NAC physisorbed in the second one. Possible reactions mechanisms for this second peak can be written as follows:

$$\overset{(-\mathrm{II})}{\mathrm{RS}} - \mathrm{Au} \rightarrow \overset{(-\mathrm{I})}{\mathrm{RS}} - \mathrm{Au} + \mathrm{e}^- \quad (11)$$

$$\overset{(-\mathrm{II})}{\mathrm{RSH_{ads}}} + \mathrm{Au} \rightarrow \overset{(-\mathrm{I})}{\mathrm{RS}} - \mathrm{Au} + \mathrm{H}^+ + \mathrm{e}^- \quad (12)$$

The resulting sulphur atoms to oxidation state (−I) ($\mathrm{RS^{\bullet}}$ or $\overset{(-\mathrm{I})}{\mathrm{RS}} - \mathrm{Au}$) recombine to give corresponding disulphide: *N*,*N*′-diacetylcystine (RSSR).

$$2\mathrm{RS}^{(-\mathrm{I})} \rightarrow \mathrm{RSSR} \quad (13)$$

The results obtained at acid and neutral pH are in agreement with those proposed by Wopschall and Shain in the case of strong adsorption reactant [38]. These authors showed that, if the reactant was strongly adsorbed, a post-peak was observed. The first peak was controlled by diffusion and corresponded to the oxidation of dissolved reductant (R) into dissolved oxidant (O) which took place through R adsorbed film ($\mathrm{R_{dissolved}} \rightarrow \mathrm{O_{dissolved}}$). The second peak (called post-peak) limited by adsorption, was present at more positive potential that first peak because of a higher stability ($\mathrm{R_{adsorbed}} \rightarrow \mathrm{O_{adsorbed}}$).

However, the involved system is more complex, as shown by experiments carried out in steady state conditions. In fact, linear correlation obtained for Koutecky–Levich equation would imply either a reactional intermediate, with the participation of the gold surface (14):

$$\begin{aligned} &\overset{(-\mathrm{II})}{\mathrm{RSH}} + \mathrm{Au} \rightarrow \overset{(-\mathrm{I})}{\mathrm{RS}} - \mathrm{Au} + \mathrm{H}^+ + \mathrm{e}^-, \\ &\overset{(-\mathrm{II})}{\mathrm{RSH}} + \overset{(-\mathrm{I})}{\mathrm{RS}} - \mathrm{Au} \rightarrow \mathrm{RSSR} + \mathrm{H}^+ + \mathrm{e}^- + \mathrm{Au} \end{aligned} \quad (14)$$

or a coupled chemical reaction (15):

$$\begin{aligned} &\mathrm{RSH_{ads}} \rightarrow \mathrm{RS^{\bullet}_{ads}} + \mathrm{H}^+ + \mathrm{e}^-, \\ &RSH_{\mathrm{sol}} + \mathrm{RS^{\bullet}_{ads}} \rightarrow \mathrm{RSH_{ads}} + \mathrm{RS^{\bullet}_{sol}}, \\ &2RS^{\bullet}_{\mathrm{sol}} \rightarrow \mathrm{RSSR} \end{aligned} \quad (15)$$

NAC electro-oxidation on gold electrode leads to *N*,*N*′-diacetylcystine dimer and not to any other sulphur species. Our conclusions are in agreement with that suggested by Feroci and Fini [2]. Indeed, they studied the reactivity between sulphur compounds and superoxide ion ($\mathrm{O_2^{\bullet -}}$), which was electrochemically generated by reduction of oxygen molecules dissolved in solution. The evolution of superoxide ion concentration, due to the presence of interacting species, was monitored by electrochemical measurements. They showed that only thiols with free –SH groups react with the superoxide ion. $\mathrm{O_2^{\bullet -}}$ has been proved to be unable to carry out oxidation of the S atom different to –SH or to achieve higher oxidation states than disulphides like sulphoxide or sulphone [2]. At contrary, these results are not in accordance with the results of others authors who claimed that thiols and disulphides can originate sulphoxides [19,20].

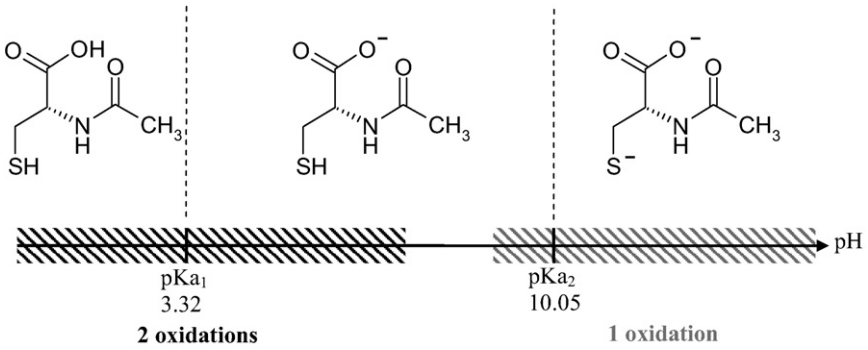

Fig. 10. Acid-basic forms of NAC with pH.

The influence of pH on NAC oxidation mechanism is shown in Fig. 10. Electrochemical behaviour of NAC depends on pH, and more precisely on the NAC acido-basic form. Moreover, the peak potential decreased when pH increased, NAC oxidation is thus facilitated at basic pH (Fig. 2). The current density for first peak decreased when pH increased and disappears completely at basic pH, where only one oxidation is observed. Molecule configuration evolves when pH increases, that being able to involve modification of NAC adsorption force. When adsorption is weak, no real difference between oxidation energies of $R_{adsorbed}$ and $R_{dissolved}$ can be considered and no post-wave is thus detected [38]. So, under basic conditions, NAC configuration changes would involve a decrease of NAC adsorption force.

Gold electrode, being used as anode, is positively charged. Under basic conditions, NAC being under the di-anion form, its electrostatic interactions with electrode surface are favoured. The missing peak controlled by diffusion can be also the consequence of an electrostatic repulsion, stronger with this pH, between adsorbed NAC and NAC in solution. Consequently, oxidation of NAC dissolved through the adsorbed layer, would not be feasible any more, contrary to acids and neutral pH.

Nevertheless, in both cases, reactions (14) and (15) remain always possible.

5. Conclusion

An electrochemical study step by step has been presented on the oxidation of NAC on gold electrode. Based on the study of the influence of several physico-chemical parameters (potential scan rate, pH, concentration, . . .) a reactional mechanism is proposed: the electrochemical reaction implies two oxidation steps including one electron and one proton. The first oxidation is diffusion-controlled whereas the second one is limited by irreversible adsorbed derivatives of NAC self-assembled monolayer. Works are now in progress concerning the regeneration of NAC by others antioxidant agents in a view to a future integration of NAC in multiphasic media like galenics.

Acknowledgements

This work was supported by Pierre Fabre dermocosmetics laboratory. The authors thank L. Massot from Laboratoire de Génie Chimique for the deconvolution of curves.

References

[1] K. Czap, Altern. Med. Rev. 5 (2000) 467.
[2] G. Feroci, A. Fini, Inorg. Chim. Acta 360 (2007) 1023.
[3] O.I. Aruoma, B. Halliwell, B.M. Hoey, J. Butler, Free Radic. Biol. Med. 6 (1989) 593.
[4] M. Liu, M. Wikonkal, D.E. Brash, Carcinogenesis 20 (1999) 1869.
[5] P.N.R. Dekhuijzen, Eur. Respir. J. 23 (2004) 629.
[6] R. Breitkreutz, N. Pittack, C.T. Nebe, D. Schuster, J. Brust, M. Beichert, V. Hack, V. Daniel, L. Edler, W. Dröge, J. Mol. Med. 78 (2000) 55.
[7] V. Valcour, B. Shiramizu, Mitochondrion 4 (2004) 119.
[8] M. Zafarullah, W.Q. Li, J. Silvester, M. Ahmad, Cell. Mol. Life Sci. 60 (2003) 6.
[9] A.-L. Fu, Z.-H. Dong, M.-J. Sun, Brain Res. 1109 (2006) 201.
[10] S. Gregory, Kelly, Altern. Med. Rev. 3 (1998) 114.
[11] S. Chevion, M.A. Roberts, M. Chevion, Free Radic. Biol. Med. 28 (2000) 860.
[12] E. Crimi, V. Sica, S. Williams-Ignarro, H. Zhang, A.S. Slutsky, L.J. Ignarro, C. Napoli, Free Radic. Biol. Med. 40 (2006) 398.
[13] R. Kohen, Biomed. Pharmacother. 53 (1999) 181.
[14] L. Gaté, J. Paul, G. Nguyen Ba, K.D. Tew, H. Tapiero, Biomed. Pharmacother. 53 (1999) 169.
[15] V. Castaignede, H. Durliat, M. Comtat, Anal. Lett. 36 (2006) 1707.
[16] A. Ruffien-Ciszak, P. Gros, M. Comtat, A.-M. Schmitt, E. Questel, C. Casas, D. Redoules, J. Pharm. Biomed. Anal. 40 (2006) 162.
[17] C. Guitton, P. Gros, M. Comtat, R. Tarroux, P. Bordat, J. Cosmet. Sci. 56 (2005) 79.
[18] J. Koryta, J. Pradac, J. Electroanal. Chem. 17 (1968) 185.
[19] J.A. Reynaud, B. Malfoy, P. Canesson, J. Electroanal. Chem. 114 (1980) 195.
[20] M.L. Hitchman, T.R. Ralph, J.P. Millington, F.C. Walsh, J. Electroanal. Chem. 375 (1994) 1.
[21] H. Han, H. Tachikawa, Frontiers Biosci. 10 (2005) 931.
[22] W.R. Fawcett, M. Fedurco, Z. Kovacova, Z. Borkowska, J. Electroanal. Chem. 368 (1994) 265.
[23] W.T. Suarez, L.H. Marcolino Jr., O. Fatibello-Filho, Microchem. J. 82 (2006) 163.
[24] Z.-N. Gao, J. Zhang, W.-Y. Liu, J. Electroanal. Chem. 580 (2005) 9.
[25] S.V. Romanenko, A.G. Stromberg, T.N. Pushkareva, Anal. Chim. Acta 580 (2006) 99.
[26] A.J. Bard, L.R. Faulkner, Electrochemical Methods: Fundamentals and Applications, second ed., Wiley, New York, 2001.
[27] A.J. Tudos, P.J. Vandeberg, D.C. Johnson, Anal. Chem. 67 (1995) 552.
[28] W. Paik, S. Eu, K. Lee, S. Chon, M. Kim, Langmuir 16 (2000) 10198.
[29] W. Yang, J.J. Gooding, D.B. Hibbert, J. Electroanal. Chem. 516 (2001) 10.
[30] M. Bieri, T. Bürgi, J. Phys. Chem. B 109 (2005) 22476.
[31] D. Chen, J. Li, Surf. Sci. Rep. 61 (2006) 445.

[32] W.R. Fawcett, M. Fedurco, Z. Kovacova, Z. Borkowska, J. Electroanal. Chem. 368 (1994) 275.
[33] W.R. Fawcett, M. Fedurco, Z. Kovacova, Z. Borkowska, Langmuir 10 (1994) 912.
[34] K. Uvdal, P. Bodö, B. Liedberg, J. Colloid Interf. Sci. 149 (1992) 162.
[35] T. Liu, M. Li, Q. Li, Talanta 63 (2004) 1053.
[36] S. Wang, D. Du, Sensors 2 (2002) 41.
[37] N. Yang, X. Wang, Q. Wan, Electrochim. Acta 51 (2006) 2050.
[38] R.H. Wopschall, I. Shain, Anal. Chem. 39 (1967) 1514.